

Magnetic QCA systems

G.H. Bernstein^{a,*}, A. Imre^a, V. Metlushko^c, A. Orlov^a, L. Zhou^a, L. Ji^a, G. Csaba^b, W. Porod^a

^aCenter for Nano Science and Technology, Department of Electrical Engineering, University of Notre Dame, Notre Dame, IN 46556, USA

^bInstitute for Nanoelectronics, TU Munich, Munich, Germany

^cUniversity of Illinois at Chicago, Chicago, IL 60607, USA

Available online 31 May 2005

Abstract

The field-coupled QCA architecture has emerged as a candidate for providing local interconnectivity for nanodevices, and offers the possibility to perform very dense, high speed, and low power computing in an altogether new paradigm. Magnetic interactions between nanomagnets are sufficiently strong to allow room-temperature operation. We are investigating the fabrication and testing of arrays of nanomagnets for this purpose, and have found that by tailoring their shapes, strong coupling can be observed. This paper will present recent work of the Notre Dame group on magnetically coupled QCA.

© 2005 Elsevier Ltd. All rights reserved.

1. Introduction

Quantum-dot cellular automata (QCA) is deemed a potential candidate to replace or supplement CMOS electronic circuits at the end of the ‘roadmap’. QCA effects computation through the interaction of fields, and requires the transfer of charge only within a small, confined volume, called a QCA cell. In most cases the fields are electrical in nature, and electrons move within a cell in response to the charge positions of neighboring cells. It has been shown theoretically [1] that an array of cells can be used to effect complex computations, similar to that of a CMOS processor.

The QCA concept [2] is independent of the material system in which it is embodied. Demonstrations of QCA logic gates [3], latches [4], and power gain [5] using metal tunnel junction technology at cryogenic temperatures have been performed. Gardelis et al. [6] have demonstrated coupled semiconductor quantum dots toward QCA. Lent [7] proposed using self assembled molecular layers for supporting charge containment, and progress toward developing the technology for building these structures is in progress [8]. DNA has been proposed by Sarveswaran et al. [9] as an alternative material for templating the molecular charge containers.

Another promising materials system, i.e. that of nanomagnetics, is the subject of this paper. The advantages of using magnetic materials to transfer information by magnetic dipoles rather than electric dipoles, as in the material systems mentioned above, include the simplicity of fabrication and robustness, for example, true room temperature operation. Additionally, magnetic materials are insensitive to radiation, suggesting applications of magnetic QCA requiring robust performance and low power consumption in harsh operating environments such as space, satellite and military applications. This paper reviews progress towards developing networks of nanomagnets suited to QCA operation, and points towards the realization of all magnetic systems, including logic, memory, and power gain.

2. Behavior of nanomagnets

As is well known, macroscale ferromagnets are composed of numerous magnetic domains, within each of which the magnetic dipoles are aligned due to quantum-mechanical exchange interactions. In the presence of a sufficiently large external field, the magnetic domains align, leading ultimately to a saturated magnetization state of the magnet. When the external field is removed, most of the domains remain aligned, and a remanent magnetization remains. This effect underlies the familiar hysteresis of $M-H$ (or $B-H$) magnetization curves, where H is magnetic field intensity, M is magnetization of the magnet, and B is the magnetic flux

* Corresponding author. Tel.: +1 574 631 6269; fax: +1 574 631 4393.
E-mail address: bernstein.1@nd.edu (G.H. Bernstein).

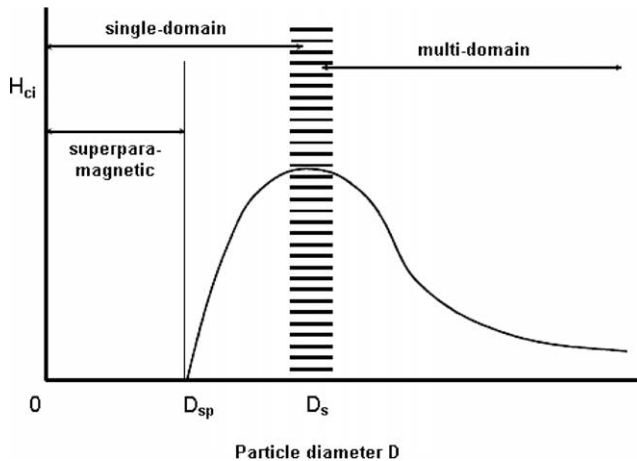


Fig. 1. Intrinsic coercivity vs. particle size.

density. Upon driving the magnet in the opposite direction, the domains reverse direction and the magnetization is reversed. At the point of zero magnetization, where no domain direction is preferred (i.e. zero crossing of the $M-H$ curve), we define the value of the external H -field as the coercive field, or the coercivity. A magnet with high coercivity is said to be ‘hard’ and one with low coercivity, ‘soft’. The value of coercivity in nanomagnets depends on their dimensions in the direction of the applied field, as well as their aspect ratio. This shape anisotropy will be shown to be critical in the application of nanomagnetics to QCA.

For simplicity, we can define a nanomagnet as one whose size is sufficiently small that the domains are relatively few, so that the behavior of the domains is somewhat predictable, controllable, and shape dependent. Fig. 1 shows the average intrinsic coercive field as a function of particle size of a collection of spherical nanomagnets [10]. For nonspherical magnets, above a critical average size, D_s depends on material, shape anisotropy, and crystal anisotropy, and the particles are multidomain. That is not to say that they are always in a multidomain configuration, but that they can be so. At and below D_s , the particles are on average single-domain and exhibit the maximum intrinsic coercivity. As the particles shrink, thermal energy, proportional to

the particle’s volume, competes with the magnetostatic energy, and the coercivity decreases. At some point, D_{sp} , thermal effects win out, the domains cannot be maintained, and the particles become superparamagnetic. For a single nanomagnet, the $M-H$ curve exhibits discrete jumps rather than smooth behavior due to the small number of individual domains [11]. Hence, the coercivity of a single particle whose size can be imagined to shrink would pass through the few-domain regime in which domain walls enable switching to occur more easily through the flipping of relatively few magnetic dipoles, to single-domain, highest coercivity state, in which no domain wall exists to nucleate switching, so that all the dipoles must flip together. Such switching of these domains can take place on time scales of a ns, which can be considered to be the upper limit to the speed of magnetic QCA.

Our dots, which range in dimensions up to about 300 nm, are somewhat larger than D_s (typically around 100 nm), but are still on the slope of the curve near D_s . By using nonspherical magnets, we can tailor the aspect ratio to provide for us a hard, i.e. short, and easy, i.e. long, axis, which allows us to define directions for coupling in the presence of an external field. As the aspect ratio of a nanomagnet increases, there is the further effect of additive magnetostatic energy and coupling along the length, so the coercivity is further increased. Hence, for a given width of magnet above D_s , longer magnets have more of a tendency to be single domain while shorter ones tend to break up into multiple domains. The following section discusses how elongated nanomagnets can be arranged to effect QCA behavior.

3. Magnetic coupling and nanomagnetic QCA

Most magnetic thin films, such as permalloy or cobalt, display in-plane magnetization. That is, the preferred domain orientation is parallel to the plane of the film. Other films, such as carefully constructed CoPt multilayers, can exhibit out-of-plane magnetization. Coupling of magnets in either of these configurations can, in principle, be

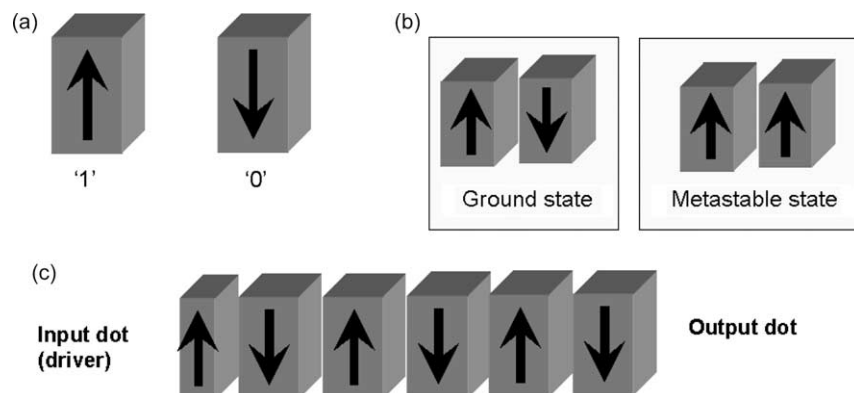


Fig. 2. (a) Definition of logic ‘1’ and ‘0’ for nanomagnets, (b) ground and metastable states for coupled pairs, and (c) QCA wire of nanomagnets.

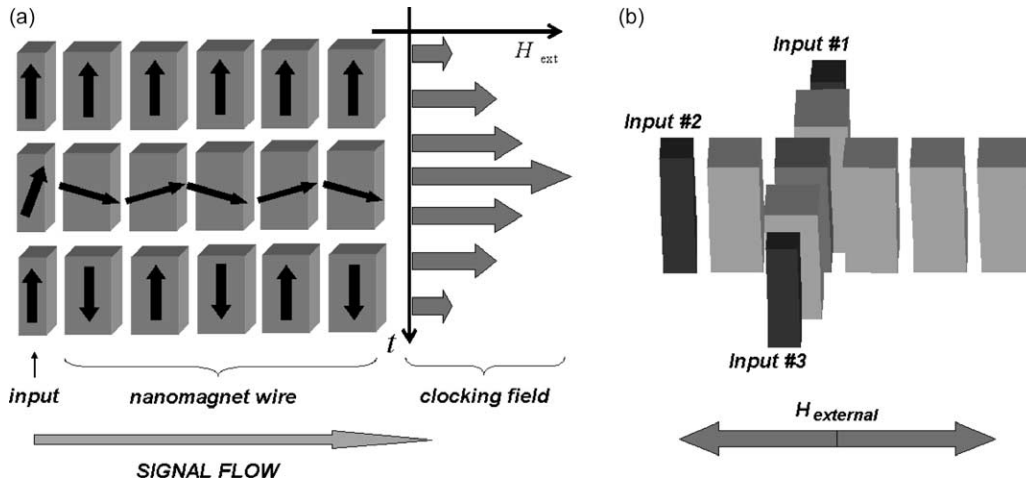


Fig. 3. Clocking of magnetic QCA devices. (a) Adiabatic clocking of QCA wire, and (b) majority gate with high coercivity input magnets (after Ref. [18]).

used for QCA [12,13]. Fig. 2(a) and (b) show how two magnets can be assigned logic states of ‘1’ or ‘0’, and can couple either in a ground state, or higher-energy metastable state. It turns out that the typical energy difference between

the two states is on the order of 100 room-temperature kT , or more, depending on the shape, size and coupling, suggesting the use of nanomagnet QCA at elevated temperatures. It is not hard to see how a chain of narrowly

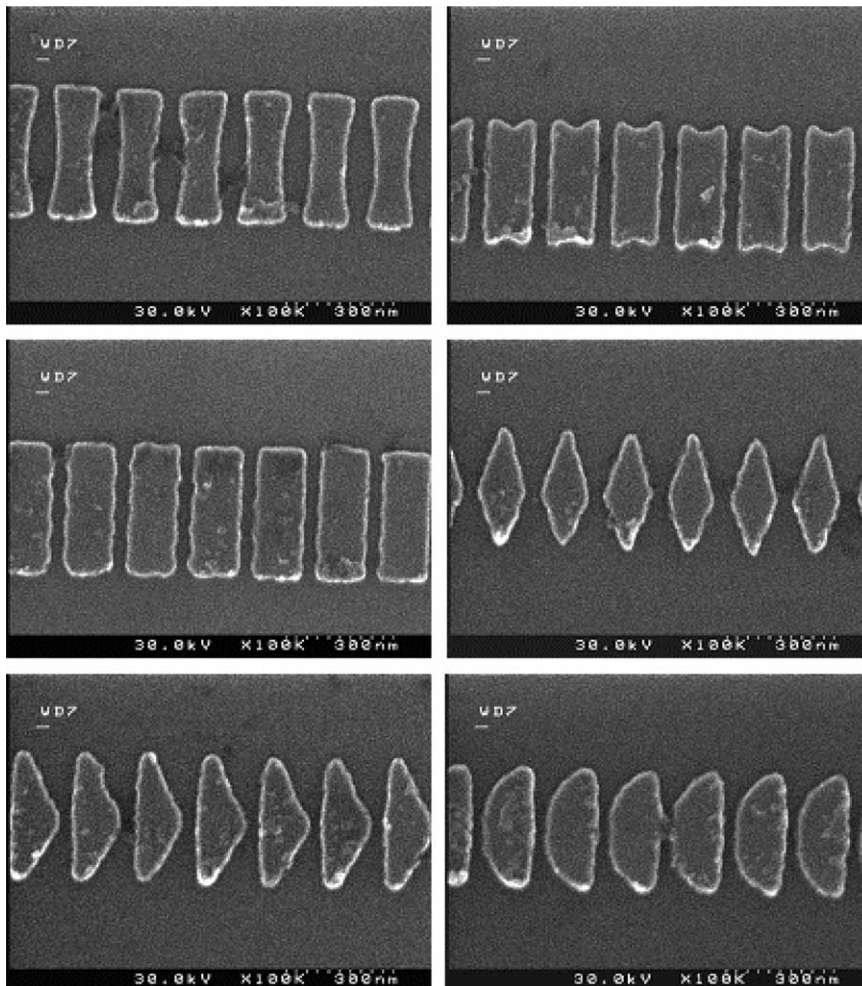


Fig. 4. Permalloy nanomagnet QCA wires featuring various shapes.

spaced nanomagnets (Fig. 2(c)) could be used as a QCA ‘wire’, as first investigated experimentally by Cowburn and Welland [14] and Cowburn [15].

Basic QCA theory involves adiabatic switching through a null state to minimize dissipation [16]. To achieve this in electronic configurations, the electrons are first allowed out of their dots within the cells by lowering the energy of their charge container walls (the manner of which depends on the chosen material system), the inputs are then applied, and finally the walls are raised adiabatically. In so doing, the array of cells remains near the ground state until the walls are fully raised and the electrons have taken on the ground state configuration with no metastable regions, or ‘kinks’, along the line.

Fig. 3(a) shows the magnetic analog of adiabatic switching, as exemplified by the switching of a QCA wire controlled by an external input and an external clocking field.

The clocking field, H_{ext} , is applied in the direction of the hard axis. As H_{ext} increases past the intrinsic coercivity of the wire components, their magnetization is forced in the same direction. However, due to shape anisotropy, the input cell having higher intrinsic coercivity retains its initial value. Power gain occurs by the energy transfer from the external clock field to the high internal energy state of the magnets (middle wire of Fig. 3(a)). This energy goes into switching as the clocking field is relaxed.

As the clock field is adiabatically lowered, the wire relaxes into the ground state with no kinks. This scheme can be extended to a majority gate, as shown in Fig. 3(b). Here, three input magnets of higher coercivity couple toward a center magnet whose magnetization is the majority vote of the three inputs, and which then is launched down the wire as in Fig. 3(a). One feature of this scheme is that it requires out-of-plane magnetization. This requires a plating process for fabrication, since conventional lift-off tends to leave conical-shaped structures as the opening in the resist at the surface closes off from the metalization. Other out-of-plane structures could be fabricated from machining multilayers of CoPt that exhibit proper magnetization direction, and such work is now in progress.

In-plane magnetization can also be used for defining QCA logic gates. We have performed extensive experiments defining variously shaped nanomagnets in order to optimize their coupling [17]. Fig. 4 shows various shapes of permalloy films fabricated by electron beam lithography [19] and liftoff.

In this figure the magnets are about 300 nm on the easy axis. In our experiments, pairs of magnets of several different aspect ratios for each shape were fabricated, magnetized, and inspected by magnetic force microscopy (MFM), a variation of atomic force microscopy (AFM) with a magnetized tip. The nanomagnet sample was magnetized by rotating in a field of 500 mT at 2000 rpm, while the field was decreased to zero over about 80 s. This scheme as a simple and inexpensive method of applying a high, but

sinusoidally varying magnetic field intended to allow the nanomagnets to relax to the ground state.

The MFM image of a single domain magnet looks like a closely coupled dark and light spot. Each pair of nanomagnets that are antiferromagnetically (AF) coupled (anti-aligned) shows light and dark spots on diagonals. Fig. 5(a) shows two trials of six different shapes, with a total of 144 pairs per shape divided among two different aspect ratios and three different sizes. The shapes are shown to the right of the MFM images. It can be seen that the larger sizes toward the top of each section are all AF coupled, while as they get smaller they are ferromagnetically coupled (aligned), as evidenced by the horizontal light and dark streaks. Careful inspection reveals that the locations of the smallest pairs that do not exhibit the desired AF coupling are mostly consistent between the two trials, suggesting that

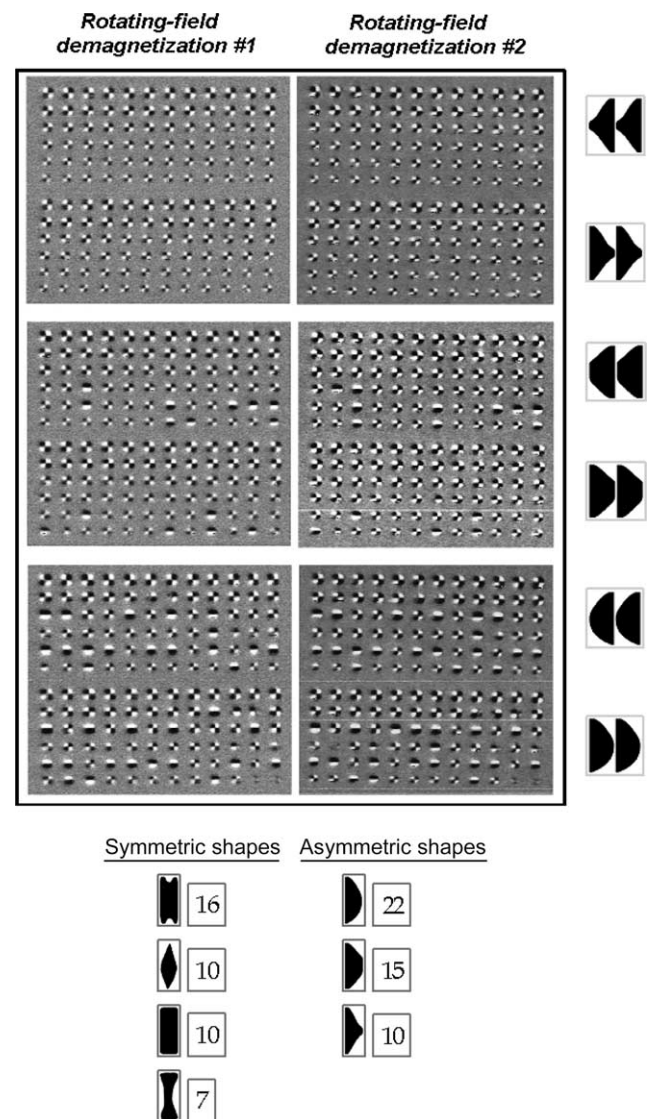


Fig. 5. MFM images of magnetic ordering of different shapes. (a) Six arrays of 144 pairs of nanomagnets of varying sizes, shapes and aspect ratios, and (b) result of statistical analysis of average coherent chain lengths of antiferromagnetically coupled magnets.

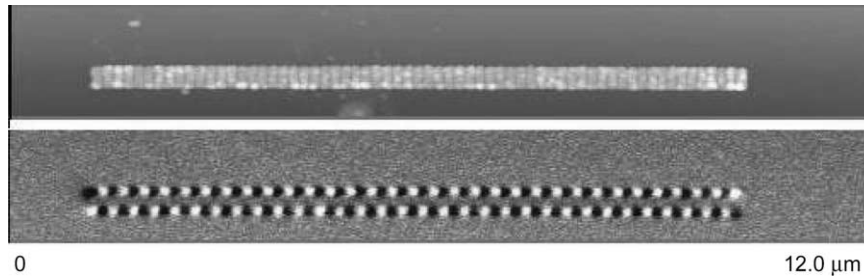


Fig. 6. Perfect antiferromagnetic ordering along a 64 magnet-long chain.

their aberrant behavior is due to defects in the fabrication process. Fig. 5(b) shows the results of a statistical analysis of errors in QCA wires for various shapes shown in Fig. 4.

The numbers represent the average ordering lengths for the different shapes, determined from the average of three independent demagnetization processes of nanomagnet chains in different sizes and aspect ratios. The average ordering length of a single chain is approximated by the length of the chain divided by the number of parallel-aligned dipole pairs in the given chain.

Fig. 6 shows the AFM and MFM images of a line of 64 rectangular magnets exhibiting perfect AF behavior down the entire line. Such strong coupling is totally outside the realm of random chance, and suggests that using nanomagnets for QCA coupling is indeed feasible. Fig. 7 shows one possible embodiment of in-plane, trapezoidal nanomagnets configured as a majority gate, as simulated by OOMMF [20]. (Parish and Forshaw [21] have modeled a similar configuration.) The three horizontal (relative to the figure) trapezoids to the left are the inputs that can be set and held at their logical values by current carrying wires during the clocking phase. As the horizontal clocking field increases, the vertical magnets are magnetized horizontally, and when the clocking field decreases, they are allowed to relax to the ground state, vertically magnetized configura-

tion. In the figure, the input magnets are all magnetized to the right, which in this case signifies a ‘1’, for the top two magnets (because of their relative configurations with the vertical direction of the coupling magnets) and a logic ‘0’ for the bottom dot. As expected, the central dot is influenced by the majority vote and is magnetized up, starting the signal propagating down the wire.

4. Summary and conclusions

We have discussed some of the interesting behavior of magnets on the nanoscale and related it to applications for quantum-dot cellular automata. We presented the utility of shape anisotropy for various configurations of nanomagnet QCA. We showed that the reliability of coupling is shape dependent, but have not yet determined the optimum shape. Simple rectangular magnets were shown in one case to couple with no errors between 64 stages. With more effort, we believe that the advantages of nanomagnet QCA, i.e. ease of fabrication, robustness at room temperature, nonvolatility, straightforward I/O, and potential integration with other magnetic systems such as magnetic random access memory (MRAM), make this a potentially useful technology in spite of its relatively low speed compared with conventional electronic devices.

Acknowledgement

This work was supported in part by grants from the Office of Naval Research, the W.M. Keck Foundation, and the National Science Foundation.

References

- [1] M.T. Niemier, P.M. Kogge, Exploring and exploiting wire-level pipelining in emerging technologies Proceedings of 28th International Symposium of Computer Architecture, Goteburg, Sweden, 2001, pp. 166–177.
- [2] S. Lent, P.D. Tougaw, W. Porod, G.H. Bernstein, Quantum cellular automata, *Nanotechnology* 4 (1993) 49–57.
- [3] I. Amlani, A.O. Orlov, G. Toth, G.H. Bernstein, C.S. Lent, G.L. Snider, Digital logic gate using quantum-dot cellular automata, *Science* 284 (1999) 289–291.

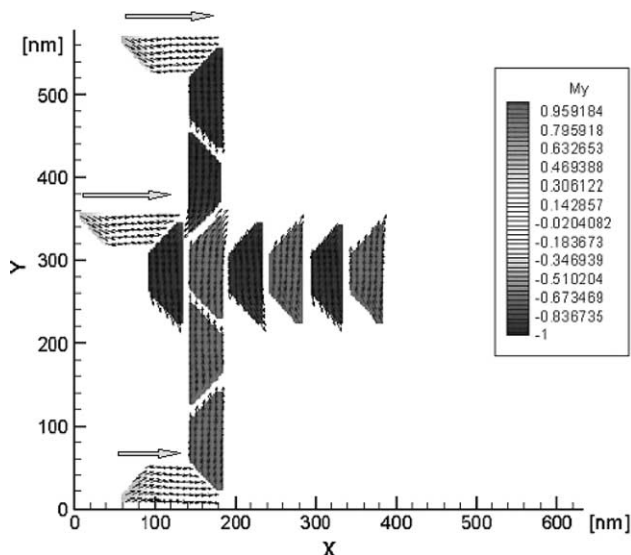


Fig. 7. OOMMF simulated result of planar majority gate.

- [4] A.O. Orlov, R.K. Kummamuru, R. Ramasubramaniam, G. Toth, C.S. Lent, G.H. Bernstein, G.L. Snider, Experimental demonstration of a latch in clocked quantum-dot cellular automata, *Appl. Phys. Lett.* 78 (2001) 1625–1627.
- [5] R.K. Kummamuru, A.O. Orlov, J. Timler, G. Toth, C.S. Lent, R. Rajagopal, G.H. Bernstein, G.L. Snider, Power gain in a quantum-dot cellular automata latch, *Appl. Phys. Lett.* 81 (2002) 1332–1334.
- [6] S. Gardelis, C.G. Smith, J. Cooper, D.A. Ritchie, E.H. Linfield, Y. Jin, Evidence for transfer of polarization in a quantum dot cellular automata cell consisting of semiconductor quantum dots, *Phys. Rev. B* 67 (2003) 033302 p. 4.
- [7] C.S. Lent, Molecular electronics—bypassing the transistor paradigm, *Science* 288 (2000) 1597–1599.
- [8] Q. Hang, Y. Wang, M. Lieberman, G.H. Bernstein, Selective deposition of molecules through polymethyl-methacrylate patterns defined by electron beam lithography, *J. Vac. Sci. Technol. B* 21 (2003) 227–232.
- [9] K. Sarveswaran, W. Hu, P. Huber, G.H. Bernstein, M. Niemier, M. Lieberman, Self-assembly and lithographic patterning of DNA rafts DARPA Conference on Foundations of Nanoscience: Self-assembled Architectures and Devices, Snowbird, Utah, April (2004).
- [10] B.D. Cullity, *Introduction to Magnetic Materials*, Addison-Wesley, 1972.
- [11] A. Hubert, R. Schafer, *Magnetic Domains*, Springer, Berlin, 1998.
- [12] G. Csaba, A. Imre, G.H. Bernstein, W. Porod, V. Metlushko, Nanocomputing by field-coupled nanomagnets, *IEEE Trans. Nanotechnol.* 1 (2002) 209.
- [13] G. Csaba, W. Porod, A.I. Csurgay, A computing architecture composed of field-coupled single domain nanomagnets clocked by magnetic field, *Int. J. Circuit Theory Applic* 31 (2003) 67.
- [14] R.P. Cowburn, M.E. Welland, Room temperature magnetic quantum cellular automata, *Science* 287 (2000) 1466.
- [15] R.P. Cowburn, Probing antiferromagnetic coupling between nanomagnets, *Phys. Rev. B* 65 (2002) 092409.
- [16] C.S. Lent, P.D. Tougaw, Device architecture for computing with quantum dots, *Proc. IEEE* 85 (1997) 541–557.
- [17] A. Imre, G. Csaba, G.H. Bernstein, W. Porod, V. Metlushko, Investigation of shape-dependent switching of coupled nanomagnets, *Superlattices Microstruct.* 34 (2003) 513.
- [18] G. Csaba, *Computing with field-coupled nanomagnets*, PhD dissertation, University of Notre Dame, 2004.
- [19] G. Bazán, G.H. Bernstein, Electron beam lithography over very large scan fields, *J. Vac. Sci. Technol. A* 11 (1993) 1745–1752.
- [20] M.J. Donahue, D.G. Porter, *OOMMF User's Guide*, Version 1.0, Interagency Report NISTIR 6376, <http://math.nist.gov/oommf/>
- [21] M.C.B. Parish, M. Forshaw, Physical constraints on magnetic quantum cellular automata, *Appl. Phys. Lett.* 83 (2003) 2046.